International Journal of Chemistry and Pharmaceutical Sciences

Journal Home Page: www.pharmaresearchlibrary.com/ijcps

Research Article **Open Access**

A vibrational spectroscopy and DFT study of 2-butyl-3-benzofuranyl 4-[2-(diethyl amino)-ethoxy]-3, 5-diiodophenyl ketone hydrochloride, amiodarone

Guillermo Diaz Fleming*, Ursula Martinez-Ortiz, Nicole Varas-Aquin

Molecular and Atomic Spectroscopy Laboratory, Department of Chemistry, Faculty of Sciences, University of Playa Ancha, Valparaiso, Casilla 34-V, Chile

A B S T R A C T

Infrared and Raman spectra of 2-butyl-3-benzofuranyl 4-[2-(diethylamino)-ethoxy]-3, 5-diiodophenyl ketone hydrochloride, amiodarone, have been recorded. Density functional theory, DFT, with the B3LYP functional was used for the optimization of the ground state geometry and simulation of the infrared and Raman spectra of this molecule. Calculated geometrical parameters fit very well with the experimental ones. Based on the recorded data, the DFT results and a normal coordinate analysis regarding a scaled quantum mechanical (SQM) force field approach, a vibrational assignment was made for the first time for this complex molecule.

Keywords: Amiodarone, Vibrational Study, DFT calculation

A R T I C L E I N F O

CONTENTS

Article History: Received 10 March 2015, **Accepted** 18 April 2015, **Available Online** 27 May 2015

***Corresponding Author**
Guillermo Diaz Fleming
Molecular and Atomic Spectroscopy Laboratory, Department of Chemistry, Faculty of Sciences, University of Playa Ancha, Valparaiso, Casilla 34-V, Chile
Manuscript ID: IJCPS2523

PAPER-QR CODE

Citation: Guillermo Diaz Fleming, et al. A vibrational spectroscopy and DFT study of 2-butyl-3-benzofuranyl 4-[2-(diethylamino)-ethoxy]-3,5-diiodophenyl ketone hydrochloride, amiodarone. *Int. J. Chem, Pharm, Sci.*, 2015, 3(5): 1665-1672.

1. Introduction

The spectroscopic techniques most widely employed in pharmaceutical research and industry include nuclear magnetic resonance (NMR) and mass spectrometry (MS). However, owing to its versatility, vibrational spectroscopy still remains a key technique in quality control laboratories and in applications where solid form characterization or minimal sample preparation is required. Owing to advances in technology and use in some specific applications, Raman spectroscopy is gaining acceptance as a powerful tool in the pharmacy field and is now becoming widely used in pharmaceutical research and development. As a consequence, vibrational spectroscopy is regularly used in the identification, characterization and investigation of pharmacologically active and related compounds as discrete materials and in formulated products.

Raman spectroscopy brings three significant advantages to pharmaceutical development compared with 'traditional' spectroscopic techniques, such as FT-IR. First, the Raman technique requires no sample preparation. Second, the coupling to an optical microscope allows the study of small particles within inhomogeneous solid sample matrices. Finally, Raman spectra can be obtained non-invasively, even within a sealed transparent container. Cardioactive agents are compounds which can selectively control either the rate or strength and rhythm of the heart beat. Antiarrhythmic drugs are those which control heart-beat rhythm and are classified on the basis of their chemical structure and intracellular electrophysiological properties [1, 2].

These kind of drugs have been widely used in the treatment of patients with heart disease in order to reduce the incidence of sudden death. However, most antiarrhythmic compounds exert varying degrees of depressant action on the haemodynamics, which limit their use, particularly in patients with compromised left ventricular function. In addition, increased mortality has been reported with the use of some antiarrhythmic agents in patients with acute coronary syndromes [3]. Since 1970s, amiodarone HCl, AMD, has been widely believed to be the most effective antiarrhythmic drug, and it has been proven to be the only antiarrhythmic agent to reduce arrhythmic death in patients with frequent ventricular ectopy postmyocardial infarction [4,5] and it has appeared to have superior efficacy to other antiarrhythmic drugs for sinus rhythm maintenance in patients with atrial fibrillation [6].

Due to the importance of AMD and further to understand the mechanisms of its actions, its crystal and molecular structures has been determined [7]. From a vibrational point of view, the FT-IR spectrum of AMD is presented in a study of solubility by complexation with β-cyclodextrin [8], while a partial FT-Raman spectrum of this compound was used in a quantitative analysis of this compound [9], where a strong band at 1568 cm^{-1} was used in the calibration process. The present work was undertaken to perform the first complete vibrational study of this drug by identifying the various normal modes with greater wave number accuracy on the basis of experimental and theoretical results, bearable to each other. The vibrational study must present evidence concerning the influence of the HCl on the tertiary amine of this molecule after forming the chlorhidrated drug. Characterization of the Infrared and Raman spectra was theoretically assisted by using Density Functional Theory (DFT) which is recognized as a powerful computational alternative to the conventional quantum chemical procedures, by inclusion of dynamic electron correlation at a much lower computational cost compared with traditional correlated methods [10-13]. The frequencies that are calculated on the basis of quantum mechanical force fields usually differ appreciably from the observed frequencies. In order to correct the systematic overestimations occurred at the calculated harmonic wave numbers which arise from the well known factors such as neglecting anharmonicity characters of the normal modes, basis set super position error, basis set truncation effect as well as the deficiencies arising from the calculation method used itself. Correction of the of the calculated force field typically uses a single factor [14] directly applied to the frequencies, so it is possible that some vibrations are affected stronger than others. A more suitable procedure to avoid this overestimation consists in using the scaled quantum mechanical force field (SQM FF) method for the prediction of the vibrational spectra.

2. Materials and Methods

Samples and instrumentation: AMD HCl of analytical grade was purchased from SUPELCO as a white crystalline solid and was used to record the Infrared and Raman spectra. FT-IR was recorded on a Buck M500 IR spectrometer equipped with a Nichrome wire-wound ceramic core and a DLATGS detector in the range 4000-600 cm^{-1}, with a resolution of 2 cm^{-1} at room temperature. IR spectra was obtained by using the KBr pellet method. Raman spectrum of the pure crystals of AMD HCl was recorded with the Advantage 200A spectrophotometer on an aluminum foil using Right Angle Input Optics accessory at room temperature. When acquiring data, the system emits up to 3 mW at 633 nm of radiation through its optics.

Computational details

Calculations for AMD were performed with the program package Gaussian 03 [15]. Density functional theory (DFT) with the B3LY functional [16) were used for the optimizations of the ground state geometries and simulation of the vibrational spectra.

The default convergence criteria and integration grid of the program were used. The basis set was the Pople's 6-31G (d) [17,18]. Vibrational spectra were obtained without anharmonic corrections and Raman activities were determined using numerical differentiation. The dominant character of each normal mode was determined by

analyzing current assignments reported in the literature for the distinct functional groups present in AMD, visual inspection of the atomic displacement of normal modes [19] as well as regarding the potential energy distribution matrix (PED) obtained from the multiple scaling of the force field calculated by the SQM method suggested by Pulay et al.[20] by using nonlinear least square scale factors to offset the systematic error produced on the theoretical frequencies [21].Transformation of Gaussian Cartesian force constants into the corresponding internal ones, conversion from Cartesian to internal coordinates, automatic generation of the redundant internal coordinates, SQM (Pulay) scaling, least-squares refinement of scale factors, and decomposition of the potential energy distribution (PED) were carried out using the program FCART01, a major modification of previous software [22].

3. Results and Discussion

Optimized structure

The optimized geometry of AMD calculated at the B3LYP/6-31G (d) level is shown in Figure 1. At the optimized structure no imaginary frequency modes were obtained, proving that a local minimum of the potential energy surface was found. Selected geometrical parameters of the distinct groups of AMD obtained at our level of theory are presented in Table 1. They show a high degree of precision with the experimental ones obtained by X-ray diffraction studies given in the literature [7].

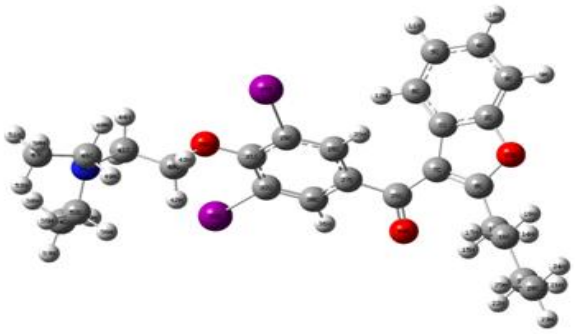

Figure 1: Optimized structure of AMD. Groups: Diethylamino Ethoxy, Diiodephenylketone,

Table 1: Selected calculated and experimental Bond distances (A) and bond angles (º) for amiodarone

Groups	**This work**	**Ref. 7**		**This work**	**Ref. 7**
Diethylamino Ethoxy					
	Bond lengths		**Bond angles**		
$N\text{-}C_{ethyl}$	1.485	1.500			
$C_{ethyl}\text{-}C_{methyl}$	1.541	1.491			
C-C (ethyl)	1.540	1.520	$O\text{-}C\text{-}C_{ethoxy}$	113.7	115.0
$N\text{-}C_{ethoxy}$	1.472	1.484	C-N-C	114.2	115.1
C-O	1.497	1.435	C-O-C	116.2	113.2
Diiodephenylketone					
$O\text{-}C_{phenyl}$	1.385	1.387			
$C\text{-}C_{I}$	1.406	1.409			
C-C	1.402	1.409			
C-I	2.147	2.111	C-C-I	119.2	116.1
$C\text{-}C_{C=O}$	1.499	-----			
C=O	1.250	1.200	$C\text{-}C\text{-}C_{\text{ketone bridge}}$	119.04	120.0
Butylbenzofuran					
$C_{co}\text{-}C_{fur}$	1.472	1.468	$(C\text{-}C)_{phenyl}\text{-}O_{co}$	123.6	118.6
C-C (ar)	1.400	1.365			
C=C (fur)	1.376	1.460			
C-C (fur)	1.368	1.356	$(C\text{-}C)_{fur}\text{-}C_{butyl}$	132.9	134.6
$O\text{-}C_{butyl}$	1.401	1.361			
$O\text{-}C_{benz}$	1.403	1.375			

C_{fur}-C_{butyl}	1.488	1.506			
C-C (butyl)	1.543	-----	$(C\text{-}C\text{-}C)_{butyl}$	111.9	113.1
C_{butyl}-C_{fur}	1.543	-----			

Vibrational Analysis:

IR and Raman Spectra

Figures 2 and 3 show, respectively, the IR and Raman spectrum of AMD HCl. AMD consists of 120 atoms with a total of 174 non redundant coordinates. These modes have been assigned taking into account the detailed vibrations of the individual atoms. Because of the complex structure of AMD, the assignment of some observed bands can be controversial. In fact, vibrational assignment for molecules containing polycyclic heteroatomic molecules is not an easy task due to the extensive coupling that occurs in the overall force field and the sheer numerical and spectral complexity of the problem as the size of the molecule increases [23]. On this ground and taking into account the different origins of these vibrations in the AMD molecule, the assignment of the distinct normal modes needs to be supported by using theoretical considerations. Also, as a way of limiting allocations of the distinct normal modes, we will briefly consider current vibrational surveys for the different groups forming part of this molecule, like benzofuran, tertiary amino ethoxy and acetophenona, as well as their alkyl and iodide derivatives, as a base to assist the final assignment. As is well documented in the literature [24-26], at about 3100-2800 cm^{-1} are expected bands concerning the aromatic C-H stretchings as well as the ethyl and butyl CH3 and CH2 stretching vibrations. In the highest part of this region are present the aromatic asymmetric and symmetric C-H stretching normal modes. The lower part concerns to CH3(ss) symmetrical stretching, CH3(ips) in-plane stretching, CH3(ops) out-of-plane stretching. For CH2 symmetric and asymmetric stretching, vibrations are usually located between the upper and lower frequencies of the corresponding CH3 normal modes.

The strong multiband absorption in the 2600-2300 cm-1 region of the tertiary amine hydrochloride salts, AMD HCl, observed in the IR spectrum by using the KBr pellet, as well as the very weak ones in the Raman spectrum, are due to vibrations involving NH+X-stretching and overtones or combination bands in Fermi resonance [25]. Further, the division of the expected broad band in this region has been explained by Warren et al. [27] as due to the reduction of hydrogen bonding of H+ to X- by the presence of water of hydratation. This fact, is evidenced in Figure 3, which shows the characteristic broad band of water centered at ca. 3500cm^{-1}. The overcrowded region between 1700-400cm^{-1}, contains bands corresponding to all molecular components of AMD. First at all, for the ketonic fragment, the well studied [28] characteristic C=O stretching band appears at 1633 (strong) and 1636 (mediun) cm^{-1} in the IR and Raman, respectively.

The ring C-C stretching vibrations give rise to characteristics bands in both the observed IR and Raman spectra, covering the spectral range from 1610–1300 cm^{-1} [29]. Thereby, about 1600-1200 cm^{-1}, Collier et al. [30-32] reported bands for benzofuran in the IR and Raman spectra, which have been assigned by Singh [33] mainly to C=C , C-C stretching and C-H in plane bending in the upper part of this region and as CO stretching modes in the lower one. The strong characteristic band reported in Ref. 9 at 1568 cm-1 in the Raman spectrum of AMDH, is found in our work at 1563 cm^{-1}, so that it can be assigned at first instance to the C=C str mode pertaining to the benzofuran part of AMDH.

Also in this region, normal modes of the alkyl moieties are present [24]. The symmetrical methyl deformation, CH3 (sd), is assigned to a medium band observed at 1330 cm^{-1} in the IR as well as in the Raman spectra, while medium bands observed at 1450 cm^{-1} in Raman and at 1437 cm^{-1} in IR spectra are attributed to the in plane methyl bending, CH3(ipb) normal mode. Bands near 1400 cm^{-1} observed in the IR and Raman spectra are attributed to the corresponding out of plane methyl bending, CH3(opb), vibration. Further, in this region the bending vibrations of methylene group found in the IR spectrum are CH2 scissoring, CH2 rocking and CH2 wagging. and CH2 twisting. The CH2 wagging and twisting modes are assigned to weak bands observed in both IR and Raman spectra at 1252 and at about 1220cm^{-1}, respectively. Bands registered at ca. 1050cm^{-1} and 1160cm^{-1} are assigned, respectively, to in plane methyl rocking , CH3(ipr) and out of plane methyl rocking, CH3(opr), modes, while the methylene rocking , CH2 (rock), mode manifests itself as a weak band registered only in the IR spectrum at ca. 690 cm^{-1} [24]. Finally, the methyl twisting, CH3 (twist), has been attributed to a medium band at ca. 400 cm^{-1} [25]. As a rule, the aromatic out-of-plane C-H deformations cover the range between 700 to 1000 cm-l [26]. For the aromatic moieties of AMD. HCl, at the nearest lower region a line at 752 crn^{-1} has been correlated with the in-phase out-of-plane benzene hydrogen wagging . Another band at 730 cm^{-1} was associated with a furan out of plane C-H bending vibration [34].

On the other hand, tertiary amines displays data by 1250-1000 cm-1 due to the antisymmetric NC3 stretchings. It is usual to observe some strong-to-medium IR band in this region, while in the Raman spectrum these frequencies are commonly observed in the 1070-1050 cm-1 and 830-740 cm^{-1} region for the antisymmetric and symmetric stretching modes, respectively [26]. Should be mentioned that the C-O stretching also can be found in this range. In the case of the larger molecules containing alkyl groups, the assignment of the C-N is not direct in the Raman spectra because of the stretching bands which arise from the carbon skeleton. Further, in this zone, an alcoxy group connected to an aromatic ring often originates two correlated lines, 1310-1210 and 1050-1010 cm^{-1} [35] . A band close to 1250 cm^{-1}

(IR very strong , Raman weak) can be considered as an aromatic carbon-oxygen stretching frequency. Another band at ca. 1040 cm-1 (IR strong, R weak), as the aliphatic carbon-oxygen stretching frequency.

The expected symmetric and asymmetric interaction between these normal modes, along with the corresponding C-O-C bending vibration, should result in a degree of mixing with ring vibrations. The allocation of the phenyl-iodide stretching vibration reported in the literature is quite ample. In Ref. 29, this normal mode has been assigned between 465 and 600cm^{-1}, while Stojiljkovid and Whiffen [36] locate this frequency will 451 cm^{-1} in p-diiodobenzene. Instead, Johnson et al. [37] write down this mode at ca. 265 cm^{-1}. It is important to take into consideration that the C-X stretching modes interact considerably with some ring modes around 1000-1200 and ca 1575 cm^{-1} of the ring vibrations [26]. In the present work, this normal mode is theoretically located at 671 cm^{-1} in the IR spectrum of AMD with some degree of mixing. Experimental, unscaled DFT and calculated multiple scaled frequencies, as well as their corresponding assignment, are reported in Table 2. For the sake of brevity, this table just present assignments concerning the most singular normal modes of the molecule under study, that is, those ones in the region between ca. 1600 and 400 cm-1 .

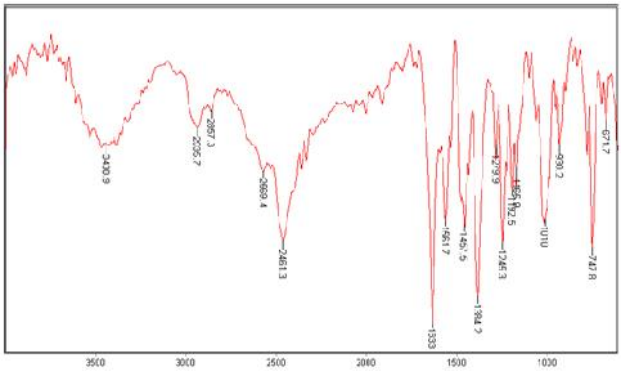

Figure 2: IR-KBr Spectrum AMD. HCl

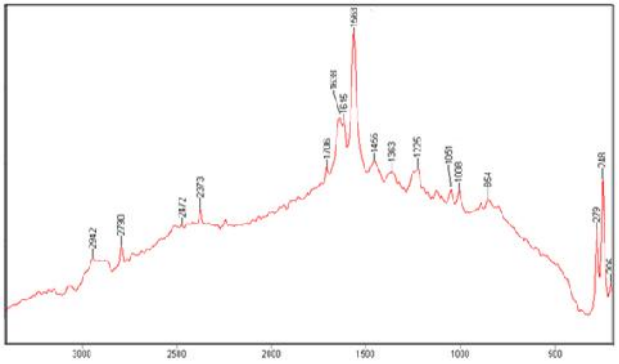

Figure 3: Raman spectrum AMD. HCl

Table 2: Selected experimental and calculated frequencies (cm^{-1})

DFT unscaled	SQM scaled	Exp. IR	Exp. Raman	Origin	Assignment
1654	1600	1633 vs	1636 m	ketone	C=O $_{str}$
1643	1594	1591 vw	1615 m	benzfur	Ring sym str + CH $_{ipb}$
1606	1557	1561 m	1563 vs	furan	C=C $_{str}$
1522	1484	1477 sh	1476 m	benzfur	CH(a) $_{ipb}$ + CH(b) $_{ipb}$
1492	1456	1457 m	1456 m	benzfur	CH(a) $_{ipb}$ + CH(c) $_{ipb}$
1469	1431	1434 sh		benzfur	CH(c) $_{ipb}$ + CH(d) $_{ipb}$
1463	1410		1416 w sh	butyl	$CH3_{opb}$
1458	1408		1408 w	ethyl	$CH3_{opb}$
1455	1402			ethyl	$CH3_{sd}$ II
1434	1396			ethoxy	$CH2_{sci}$
1423	1393			ethyl	$CH2_{sci}$ I
1421	1389			ethyl	$CH2_{sci}$ II
1411	1380	1384 s		ethoxy	$CH2_{sci}$
1399	1371		1363 w m	butyl	CH3 $_{asd}$
1384	1353			ethyl	CH2 $_{wag}$ I
1381	1352			butyl	CH2 $_{sci}$ + $CH3_{sd}$
1376	1341		1340 mw	ethoxy	CH2 $_{twist}$
1368	1337			ethyl	$CH2_{twist}$ II
1364	1336			butyl	CH2 $_{sci}$ + CH3 $_{asd}$
1358	1322			butyl	CH2 $_{wag}$
1352	1321			ethyl	$CH2_{twist}$ II + CH3 $_{asd}$
1350	1317			butyl	CH2 $_{twist}$ + CH3 $_{asd}$
1348	1316	1311 vw	1316 w	ethyl	CH2 $_{wagg}$ I, II
1341	1306			benzfur	In plane def + CH $_{ipb}$
1322	1296	1279 m	1296 w	ethyl	$CH2_{twist}$ II
1301	1270			butyl	CH2 $_{twist}$
1299	1257			butyl-benzfur	$CH2_{twist}$ + ring def
1285	1254	1245 ms	1245 m	ethyl	CH2 $_{wagg}$ I, II
1257	1226	1222 sh	1225 m	ethyl	$CH2_{twist}$ I,III

1252	1221			ethoxy	C-O $_{str}$
1251	1218			ethyl	$CH2_{rock}$
1248	1213			benzfur	CH_{ipb}
1236	1205			phen	C-CO $_{str}$
1216	1182	1192 m		phen	C-C + CCO
1200	1175	1172 m		benzfur	$C\text{-}H_{ipb}$
1199	1168	1165 w m		benzfur	C-H $_{ipb}$ + benz def
1173	1144			butyl	CH3 $_{opr}$
1157	1134			benzfur + but	C-H $_{ipb}$ + CH2 $_{rock}$
1141	1117		1125 w	amine	C-N $_{str}$
1128	1104			butyl	C-C $_{str}$
1127	1103			benzfur	asym def
1109	1086	1099 w	1105 w	ethyl	$CH2_{rock}$
1105	1079			ethyl	$CH3_{ipr}$ + $CH2_{twist}$
1096	1074			butyl	$CH3_{bend}$ + CH2 $_{twist}$
1082	1049	1057 mw	1051 mw	phen	Ring in plane def + C-I $_{str}$
1059	1025	1027 sh		amine-ethoxy	C-N-C $_{asym\ str}$ I
1045	1017			amine-ethoxy	C-N-C $_{asym\ str}$ II
1040	1012	1010 s	1008 w	ethoxy	C-N-C $_{asym\ str}$
1027	1003	1001 ms		butyl	C-C-C $_{asym\ str}$
1023	995			benzfur	CH $_{opb\ asym}$
1006	988			amine	(NC3) $_{asym\ str}$
994	973	989 sh	973 w	phen	C-H $_{opb}$
989	972			butyl	C-C $_{str}$
987	963			ethyl	C-C $_{str}$ I, II
981	957	955 mw	957 w	phen, benz	C-H $_{opb}$
977	954			butyl, phen	C-C $_{strt}$ + C-H $_{opb}$
963	941			phen	Ring trigonal bend + $C\text{-}H_{opb}$
962	929	930 mw		phen	Ring breath + $O\text{-}C_{str}$
918	901	921 sh		ethoxy	O-C $_{str}$
898	898		913 w	amineethoxy	N-C $_{str}$ + C-C $_{str}$ I,II
864	895		893 w	benzfur, but	C-O $_{sym\ str}$ + C-C $_{str}$
863	885		873 w	benzfur, but	C-O $_{asym\ str}$ + C-C $_{str}$
850	844	853 w	849 mw	benzfur	Ring in plane def
839	842			phen	Ring in plane def
835	834	836 w		benzfur	Ring in plane def
829	821			ethyl	$CH3_{rock}$ I + $CH2_{rock}$ II
818	817			butyl	$CH3_{rock}$ + $CH2(1)_{rock}$
810	811			ethyl	$CH3_{rock}$ II + $CH2_{rock}$ I
794	802		802 w	ethoxy	$CH2_{rock}$
776	795		793 w	butyl	$CH2(1)_{rock}$ + $CH2(2)_{rock}$
757	778	777 m		ethyl	$CH3_{rock}$ + $CH2_{rock}$ I II
752	763			benzfur	Ring Out of plane def + CH $_{opb}$
741	745	747 s		benzfur	CH $_{opb}$
736	739			butyl	$CH2\ (3)_{rock}$
715	729			amine	(N-C)3 $_{sym\ str}$
692	721			phen	Ring in plane def
655	701	700 w		furan	Ring out of plane def
617	678	671 w	654 w	phen	Ring in-plane def + C-I $_{strt}$
593	649	637 sh		benzfur, phen	Ring in-plane def
587	605	607 mw		benzfur	Ring in plane def + C-H $_{opb}$
547	584			benzfur, phen	Ring out of plane def
541	575			benzfur, phen	Ring out of plane def
525	535			benzfur, ketone	Ring o-of-plane def + C-O-C $_{bend}$
520	532			phen	Ring out of plane def
500	516			acetophen	C-C-CO $_{bend}$
466	514			amine	C-N-C $_{bend}$
465	494			ethoxy-phen	C-O-C $_{bend}$
429	459			amine	N-C-C $_{bend}$
406	456			butyl	$CH3_{twist}$

391	422	amine	C-N-C-C_{tors} I,II
380	401	amine	C-N-C-C_{tors} II,III
357	385	butyl	C-C-C-C_{tors}

Abbreviations. bend: bending; w: weak; s: strong; m: medium; sh:shoulder;sd: symmetric deformation; opb.: out-of-plane bending; ipb: in-plane bending ; sym str: symmetric stretching; asym str: asymmetric stretching; tors: torsion; wag: wagging; sci: scissoring; rock: rocking; twist: twisting; phen:phenylcetone; benzfur:benzofuran. Numbers in parenthesis 1, 2, 3, distinguish the CH2 groups in butyl fragment. Letters a, b.c. d in parenthesis indicate different C-H in benzofuran. I, II concern distinct ethyl groups.

4. Conclusion

Combining quantum chemical results and normal coordinate analysis with IR and Raman literature data, it has been possible to perform a vibrational frequency assignment with a suitable degree of confidence for such a complex molecule like AMD. This detailed band assignment is performed for the first time for this molecule and will be useful for the in situ identification as well as for future and pharmacological studies of this important drug. The DFT level of calculation used in the present work together with the SQM treatment has proven to be an appropriate tool to support the assignment of the distinct normal modes of AMD.

5. Acknowledgment

GDF and UMO acknowledge DGI Universidad de Playa Ancha (Project DGI 01-14-15).

6. References

1. B.N. Singh, E.M. Vaughan Williams, Br. J. Pharmacol. **1970**, 39: 657-667
2. B.N. Singh, L.H. Opie, D..C. Harrison, I.F. Marcus, (**1987**). Drugs for the Heart, edited by L. H. Opie, pp. 54-90.
3. Orlando: Grune & Stratton.The Cardiac Arrhytmia Suppression Trial (CAST) Investigators, Preliminary Report: Effect of Encainide and Flecainide on Mortality in Randomized Trial of Arrhytmia Suppression after Myocardial Infarction, N. Engl. J. Med. **1989**, 321: 406-412
4. J.A. Cairns, S.J. Connolly, R. Roberts, M. Gent, Randomized Trial of outcome after myocardial infarction in patients with frequent or repetitive ventricular premature depolarisations:CAMIAT, Lancet. **1997**, 349: 675-682
5. B.M. Massie., S.G. Fisher, M. Randford, Effect of amiodarone on clinical status and left ventricular function in patients with congestive heart failure. CHF.STAT Investigators, Circulation, **1996**, 93: 2128-2134
6. S. Mattel, Newer developments in the management of atrial fibrillation, Am.Heart J. **1995**, 130: 1094-1106
7. V. Cody, J..Luft, Acta Cryst. **1989**, B45: 172-178
8. M. K. Rieke, M. P. Tagliari, A. Granada , G. Kuminek, M. A. Segatto-Silva, H. K.Stulzer, Materials Science and Engineering C, **2010**, 30: 1008-1013
9. M.G. Orkoula, C.G. Kontoyannis, C.K. Markopoulou, J.E. Koundourellis, Talanta, **2007**, 73: 258-261
10. P. Hohenberg, W. Kohn, Inhomogeneous electron gas, *Phys. Rev.* **1964**, 136: B864-B871
11. M. Levy, Proc. Natl. Acad. Sci. USA, **1979**, 76: 6062-6065
12. G. Vignale , M. Rasolt, Density-functional theory in strong magnetic field, Phys. Rev. Lett., **1987**, 59: 2360-2363
13. W. Kohn, L. J. Sham, Self-consistent equations including exchange and correlation effects, Phys. Rev. 1965, 140: A1133-1138
14. A.P. Scott, L. Radom, J. Phys. Chem. **1996**, 100: 16502-16513
15. Gaussian 03, Revision C.02, 1. Frisch MJ, Trucks GW, Schlegel HB, Scuseria GE, Robb MA, Cheeseman JR, J. A. Montgomery J, Vreven T, Kudin KN, Burant JC, Millam J M, Iyengar SS, Tomasi J, Barone V, Mennucci B, Cossi M, Scalmani G, Rega N, Petersson GA, Nakatsuji H, Hada M, Ehara M, Toyota K, Fukuda R, Hasegawa J, Ishida M, Nakajima T, Honda Y, Kitao O, Nakai H, Klene M, Li X, Knox JE, Hratchian HP, Cross JB, Bakken V, Adamo C, Jaramillo J, Gomperts R, Stratmann RE, Yazyev O, Austin AJ, Cammi R, Pomelli C, Ochterski JW, Ayala PY, Morokuma K, Voth GA, Salvador P, Dannenberg JJ, Zakrzewski VG, Dapprich S, Daniels AD, Strain MC, Farkas O, Malick DK, Rabuck AD, Raghavachari K, Foresman JB, Ortiz JV, Cui Q, Baboul AG, Clifford S, Cioslowski J, Stefanov BB, Liu G, Liashenko A, Piskorz P, Komaromi I, Martin RL, Fox DJ, Keith T, Al-Laham MA, Peng CY, Nanayakkara A, Challacombe M, Gill PMW, Johnson B, Chen W, Wong MW, Gonzalez C, Pople JA, Gaussian, Inc., Wallingford CT, **2004**.
16. A.D. Becke, J. Chem. Phys. **1993**, 98: 5648-5652
17. C. Lee, W. Yang, R.G. Parr, Phys. Rev. B: Condens. Matter, **1988**, 37: 785-789
18. R. Ditchfield, W.J. Hehre, J.A. Pople, J. Chem. Phys. **1971**, 54: 720-723
19. GAUSSVIEW Users Manual, A. Frisch, A. B. Nielsen, A. J. Holder, Gaussian Inc, **2000.**
20. P. Pulay, G. Fogarasi, G. Pongor, J.E. Boggs, A. Vargha, J. Am. Chem. Soc., **1983**, 105: 7037-7047

21. J.B. Foresman, A. Frisch, Exploring Chemistry with Electronic Structure Methods, 2nd ed., Gaussian Inc., Pittsburgh, PA, **1996**.
22. W.C. Collier, QCPE Bull., **1996,** 13: 16502
23. G. Zerbi, in A.J. Barnes and W.J. Orville-Thomas (Eds.), Vibrational Spectroscopy-Modem Trends, Elsevier, New York, **1977**.
24. G. Socrates, Infrared and Raman Characteristic Group Frequencies: Tables and Charts, 3rd ed., John Wiley & Sons, New York/Brisbane/ Weinheim/Singapore/Toronto, **2004**.
25. N. B. Coltup, L. H. Daly and S. E. Wiberley, Introduction to Infrared and Raman Spectroscopy, 3rd. Ed. Academic Press (**1990**).
26. D.L. Vien, N.B. Colthup, W.G. Fateley, J.G.Grasselli., The Handbook of Infrared and Raman Characteristic Frequencies of Organic Molecules, Academic Press, Boston, **1991**.
27. R. J. Warren, W. E. Thompson, and J. E. Zarembo, J. Pharm. Sci., **1965**, 54: 1554
28. B. Smith, Infrared Spectral Interpretation, A Systematic Approach, CRC Press, Washington, DC, **1999**.
29. L.J. Bellamy, the Infrared Spectra of Complex Molecules, John Wiley & Sons, New York, **1975**.
30. W.B. Collier, T.D. Klots, Spectrochim. Acta Part A, **1995**, 51: 1255-1272
31. T.D. Klots, W.B. Collier, Spectrochim. Acta Part A, **1995**, 51: 1291-1316
32. W.B. Collier, I. Klots, T.D. Magdo, J. Chem. Phys., **1999**, 110: 5710-5720
33. V.B. Singh, Spectrochim. Acta, **2006**, 65: 1125-1130
34. A. Hirakawa, Y. Nishimura, T. Matsumo, M. Nakanishi and M. Tsuboi, J. Raman Spectrosc. , **1978**, 7: 282-287
35. A.R. Katritzky and N.A. Coats, J. Chem. Soc. London p. **1959**, 2062.
36. A. Stojiljkovid and D. H. Whiffen Spectrochim. Acta, **1958**, 47-56
37. B. R. Johnson, C. Kittrell, P. B. Kelly, J. L. Kinsey**,** J. Phys. Chem., **1996**, 100: 7743-7764.